Prediction of Fan Tone Radiation Scattered By A Cylindrical Fuselage

To cite this article: D-M. Rouvas and A. McAlpine 2022 *IOP Conf. Ser.: Mater. Sci. Eng.* **1226** 012050

Prediction of Fan Tone Radiation Scattered By A Cylindrical Fuselage

D-M. Rouvas and A. McAlpine

Institute of Sound and Vibration Research, University of Southampton, Southampton, SO17 1BJ, United Kingdom

E-mail: D-M.Rouvas@soton.ac.uk

Abstract. A theoretical prediction method of the scattering of fan tone radiation from a turbofan inlet duct by the airframe fuselage is presented. The fan tone noise is modelled by an acoustic disc source that represents the sound field at the inlet duct termination. Adjacent to the source is a cylindrical fuselage that scatters the fan tone radiation. The prediction method is valid for upstream sound radiation. The acoustic pressure on the cylindrical fuselage is affected by refraction of the sound as it propagates through the fuselage boundary layer. This effect known as boundary layer shielding is more prominent forward of the turbofan, since the fan tone noise radiated from the inlet duct is propagating upstream. An asymptotic approach is used to model sound propagation through a boundary layer which is modelled by a thin linear shear velocity profile. Consequently the scattered pressure field can be computed very quickly, thus providing a fast and efficient prediction method. Although a realistic fuselage turbulent boundary layer does not resemble a linear shear layer, it is shown that the effect of acoustic shielding by a turbulent boundary layer can be modelled by taking a liner shear profile with a shape factor that matches the shape factor for a realistic turbulent profile.

1. Introduction

The introduction of the turbofan engine caused a significant decrease in the intensity of jet noise, but increased the prominence of fan noise. With the ongoing development of ultra high-bypass-ratio turbofan engines, the prominence of fan noise is expected to become more dominant compared to other noise sources on an aircraft. However, it can be misleading to examine the fan noise source radiating in a free-field as highlighted by previous research ([1], [2], [3]). Calculating the propagation of fan noise in the free field is not sufficient because the interaction of the source with the rest of the airframe, especially the adjacent fuselage, can alter substantially the acoustic pressure field. Thus the modelling of acoustic installation effects for engine noise sources is important to provide more accurate predictions than the free-field response.

The aim of the work presented here is to develop theoretical methods to predict the scattering and refraction of fan tone radiation owing to the presence of a cylindrical fuselage adjacent to the turbofan engine. Specifically, analytic expressions that describe the acoustic pressure near- and far-field of an installed fan tone noise source adjacent to a cylinder have been derived and benchmarked. The fan tone noise source is modelled by a distribution of monopoles on a disc that simulates a spinning mode exiting a turbofan inlet duct, as proposed by McAlpine et al. [4]. By calculating both near- and far-field, the methods can be applied to the evaluation of both cabin and ground noise.

Previous research on this problem relied on numerical methods to calculate sound propagation through the fuselage boundary layer (for example McAninch [5], Tam and Morris [6], Hanson and Magliozzi [2], McAlpine, Gaffney and Kingan [4], Gaffney, McAlpine and Kingan [7]). This is of key importance for upstream sound propagation which via boundary layer refraction effects can be 'shielded' from the fuselage's surface [1].

McAninch [5] and Tam and Morris [6] were the first researchers to solve the Pridmore-Brown equation to model sound refraction effects by the fuselage boundary layer. They proposed a numerical scheme utilizing a Frobenius series in order to bridge the singularity that is present in the Pridmore-Brown equation. Subsequently, Hanson and Magliozzi [2] were the first to model the scattered field from a propeller source adjacent to a cylindrical fuselage. In fact, the propeller source model was the only one available until McAlpine et al. [4] and Gaffney [7] introduced a model that simulates fan tones radiated from a turbofan inlet duct.

In this paper, sound propagation in the boundary layer region is determined via an asymptotic method proposed by Eversman and Beckemeyer [8], leading to an analytical formulation that only requires numerical evaluation of an inverse Fourier transform to obtain the near-field acoustic pressure. Consequently the near-field pressure can be computed very quickly, thus providing a fast and efficient prediction method. Although not presented in this paper, the same approach has been employed to derive an analytic expression for the far-field pressure. In fact, in the far field the inverse Fourier transform can be evaluated using the method of stationary phase, leading to a fully analytical result.

2. Theoretical Background and Analysis

The analysis in § 2.1 and § 2.2 follows the procedure in McAlpine et al. [4]. Full details of the analysis in § 2.3 for the linear boundary layer is in Rouvas and McAlpine [9].

2.1. In-duct Sound Field

Consider a ducted fan in a cylindrical inlet duct of radius a. The cylindrical coordinate system (r, ϕ, z) has its z-axis coincident with the duct's centerline. A subsonic uniform flow of Mach number $M_z = U_z/c_0$ is directed in the negative z-direction. As described in McAlpine et al. [4], a time-harmonic spinning mode, exiting the duct with azimuthal order l and radial order q, has acoustic pressure and axial particle velocity given by

$$\hat{p}_{lq} = P_{lq} \mathrm{J}_l(\kappa_{lq} r) \mathrm{e}^{\mathrm{i}(-l\phi - k_{zlq} z)} \quad \text{and} \quad \hat{u}_{zlq} = \frac{\xi_{lq}}{\rho_0 c_0} P_{lq} \mathrm{J}_l(\kappa_{lq} r) \mathrm{e}^{\mathrm{i}(-l\phi - k_{zlq} z)}, \tag{1}$$

where P_{lq} is the modal amplitude, $\xi_{lq} = \frac{k_{zlq}}{(k_0 + k_{zlq} M_z)}$, and the dispersion relationship is given by $k_{zlq}^2 + \kappa_{lq}^2 = (k_0 + k_{zlq} M_z)^2$. Also, κ_{lq} is the set of eigenvalues which satisfy $\mathrm{J}_l'(\kappa_{lq} a) = 0$, k_{zlq} is the axial wavenumber of mode (l, q), c_0 is the speed of sound, ρ_0 is the mean density of the air inside the duct, and the freespace wavenumber $k_0 = \omega_0/c_0$.

2.2. Uniform Flow Analysis

The derivation of the total field when the flow is uniform is taken from McAlpine et al. [4]. Here only a brief outline is provided. Adjacent to the source, there is a cylindrical fuselage. Another cylindrical coordinate system $(\bar{r}, \bar{\phi}, \bar{z})$ is used, with its $\bar{z}$-axis coincident with the fuselage's centerline. The perpendicular distance between the z-axis and the $\bar{z}$-axis is b. Then Graf's Addition Theorem is used in order to express the incident field in terms of the cylindrical coordinate system centered on the fuselage rather than on the duct's centerline, as described in Refs. [2], [7], [10]. The incident field expression is given for $\bar{r} < b$ (near-field)

$$\overline{p'_{in}}(\bar{r}, k_z, t) = \pi^2 \xi_{lq} P_{lq} (-1)^{l+n} (k_0 + k_z M) \, \Psi_{lq} \, \mathrm{e}^{-\mathrm{i}(l-n)\beta} \, \mathrm{H}_{l-n}^{(2)}(\Gamma_0 b) \, \mathrm{J}_n(\Gamma_0 \bar{r}) \, \mathrm{e}^{\mathrm{i}\omega_0 t}, \tag{2}$$

where $\Gamma_0^2 = (k_0 + k_z M_z)^2 - k_z^2$ is a radial wavenumber, and the function Ψ_{lq} is given by

$$\Psi_{lq} = \frac{\Gamma_0 a}{\kappa_{lq}^2 - \Gamma_0^2} \mathrm{J}_l(\kappa_{lq} a) \mathrm{J}_l'(\Gamma_0 a), \quad \Gamma_0 \neq \kappa_{lq}, \tag{3}$$

$$\Psi_{lq} = \frac{1}{2}\left(a^2 - \frac{l^2}{\kappa_{lq}^2}\right) \mathrm{J}_l^2(\kappa_{lq} a), \quad \Gamma_0 = \kappa_{lq}. \tag{4}$$

Note that $\overline{\cdot}$ denotes a Fourier-transformed variable.

An alternative expression can be derived for $\bar{r} > b$ which is used for the far-field result.

Since the scattered waves take the form of the scattering surface, the scattered field is formed of cylindrical outward propagating waves. Thus the Fourier-transformed scattered field is expressed in terms of a Hankel function as shown in Ref. [4].

It immediately follows that the Fourier-transformed total field can be constructed by summing the Fourier-transformed incident and scattered fields, with the scattered field determined such that the total field satisfies a hard-wall boundary condition at the fuselage surface ($\bar{r} = a_0$).

For the near-field case, the acoustic pressure at the fuselage surface is of interest because it enables the evaluation of cabin noise. On setting $\bar{r} = a_0$, and performing an inverse Fourier $\bar{z}$-transform, the total pressure on the fuselage surface in real space is obtained

$$p_t'(a_0, \bar{\phi}, \bar{z}, t) = \frac{\xi_{lq} P_{lq}}{4} (-1)^l \, \mathrm{e}^{-\mathrm{i}l\beta} \, \mathrm{e}^{\mathrm{i}\omega_0 t} \sum_{n=-\infty}^{\infty} \left\{ (-1)^n \, I_n(a_0, \bar{z}) \, \mathrm{e}^{-\mathrm{i}n(\bar{\phi}-\beta)} \right\}, \tag{5}$$

where

$$I_n(a_0, \bar{z}) = \int_{-\infty}^{\infty} (k_0 + k_z M) \, \Psi_{lq} \, \mathrm{H}_{l-n}^{(2)}(\Gamma_0 b) \left[\left(-\mathrm{i}(2/\pi\Gamma_0 a_0) \right) / \mathrm{H}_n^{(2)\prime}(\Gamma_0 a_0) \right] \mathrm{e}^{-\mathrm{i}k_z \bar{z}} \, \mathrm{d}k_z. \tag{6}$$

The inverse Fourier $\bar{z}$-transform integral cannot be solved analytically, and therefore a numerical integration routine must be employed.

2.3. Linear Boundary Layer Profile Analysis

As already mentioned, previous researchers emphasised the importance of boundary-layer refraction effects on upstream sound propagation. Experimental data [2] showed a discrepancy between the sound levels measured upstream of the source compared with theoretical predictions. This was because the predictions assumed uniform flow and did not take into account the boundary layer. The problem of sound propagation through a shear layer, such as a boundary layer, requires the solution to the Pridmore-Brown equation [11]. The Fourier-transformed Pridmore-Brown equation in terms of cylindrical coordinates is

$$\frac{\mathrm{d}^2 \overline{p_{t_{in}}'}}{\mathrm{d}\bar{r}^2} + \left(\frac{1}{\bar{r}} - \frac{2k_z M'}{k_0 + k_z M} \right) \frac{\mathrm{d}\overline{p_{t_{in}}'}}{\mathrm{d}\bar{r}} + \left[(k_0 + k_z M)^2 - k_z^2 - \frac{n^2}{\bar{r}^2} \right] \overline{p_{t_{in}}'} = 0. \tag{7}$$

Previous researchers ([2], [5], [6], [7], [10]) used numerical methods to solve this equation.

Eversman and Beckemeyer [8] proposed an asymptotic approach to solve eq. (7). The work presented here uses this approach to solve the problem of sound propagation inside a linear boundary layer profile with slip velocity at the wall, as shown sketched in Fig. (1). Again here only a brief outline is provided. Following Eversman and Beckemeyer, introduce the change of variables $y = \frac{\bar{r} - a_0}{a_0}$ and $\zeta = \frac{y}{\varepsilon}$, with the parameter $\varepsilon = \frac{\delta}{a_0}$ the non-dimenional boundary layer

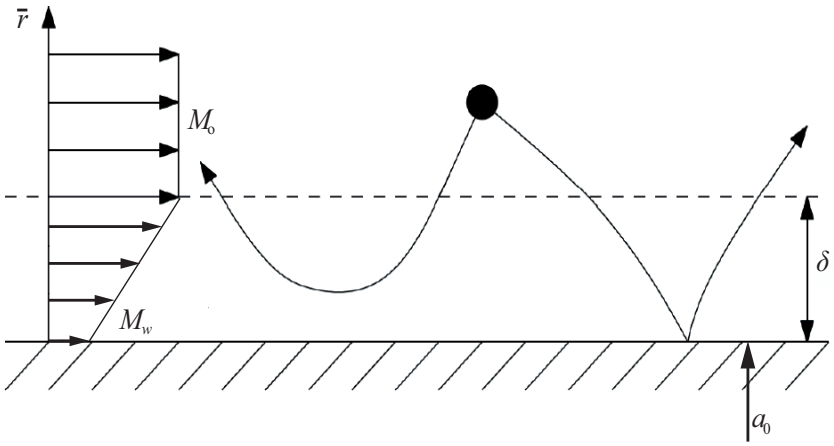

Figure 1. Boundary layer with linear velocity profile.

thickness. The Pridmore-Brown equation is then solved for small values of the parameter ε by assuming a power series solution [8]

$$\overline{p'_{t_{in}}}(\zeta) = \overline{p'_0}(\zeta) + \varepsilon\overline{p'_1}(\zeta) + \varepsilon^2\overline{p'_2}(\zeta) + \varepsilon^3\overline{p'_3}(\zeta) + \dots . \tag{8}$$

Substituting eq. (8) into eq. (7), and also the equation that specifies the hard-wall boundary condition, yields a set of equations that can be solved to give the terms of the power series $\overline{p'_0}(\zeta)$, $\overline{p'_1}(\zeta)$, $\overline{p'_2}(\zeta)$ etc. It is noted that sufficient accuracy is achieved by taking up to second order as shown in Rouvas and McAlpine [9]. Thus, the pressure and its derivative inside the boundary-layer are obtained in the form given by eq. (8).

The pressure field outside the boundary layer is the solution to the inhomogeneous convected wave equation, since the flow is assumed uniform everywhere except in the boundary-layer region. The Fourier-transformed total field outside the layer will be the sum of the incident field, given by eq. (2), and the scattered field. By employing matching conditions at the edge of the boundary layer, namely continuity of pressure $\overline{p'_{t_{in}}}(\zeta = 1) = \overline{p'_{i_{out}}}(\bar{r} = a_0 + \delta) + \overline{p'_{s_{out}}}(\bar{r} = a_0 + \delta)$, and continuity of particle displacement, which is equivalent to continuity of pressure gradient, $\frac{\mathrm{d}\overline{p'_{t_{in}}}}{\mathrm{d}\bar{r}}(\zeta = 1) = \frac{\mathrm{d}\overline{p'_{i_{out}}}}{\mathrm{d}\bar{r}}(\bar{r} = a_0 + \delta) + \frac{\mathrm{d}\overline{p'_{s_{out}}}}{\mathrm{d}\bar{r}}(\bar{r} = a_0 + \delta)$, the problem can be solved to determine the Fourier-transformed total field inside and outside the boundary layer.

Finally, by performing an inverse Fourier $\bar{z}$-transform, the total pressure at the fuselage surface, i.e. $\overline{p'_{t_{in}}}(\zeta = 0)$, is given by

$$p'_{t_{in}}(a_0, \bar{\phi}, \bar{z}, t) = \frac{\xi_{lq} P_{lq}}{4}(-1)^l \mathrm{e}^{-\mathrm{i}l\beta} \sum_{n=-\infty}^{\infty} (-1)^n \mathrm{e}^{\mathrm{i}n\beta} I_n^{(lbl)}(a_0, \bar{z}) \mathrm{e}^{-\mathrm{i}n\bar{\phi}}\, \mathrm{e}^{\mathrm{i}\omega_0 t}, \tag{9}$$

where

$$I_n^{(lbl)}(a_0, \bar{z}) = \int_{-\infty}^{\infty} (k_0 + k_z M_0)\, \Psi_{lq}\, \mathrm{H}^{(2)}_{l-n}(\Gamma_0 b)\, S_n(k_z, \omega_0) \mathrm{e}^{-\mathrm{i}k_z \bar{z}}\, \mathrm{d}k_z, \tag{10}$$

and

$$S_n(k_z, \omega_0) = \Bigg[\mathrm{J}_n(\Gamma_0(a_0 + \delta)) \frac{1}{G} + \frac{\left[\mathrm{J}'_n(\Gamma_0(a_0 + \delta)) - \frac{R}{G} \frac{\varepsilon}{\Gamma_0 a_0} (1 + KM_0)^2 \mathrm{J}_n(\Gamma_0(a_0 + \delta)) \right]}{\left[\frac{R}{G} \frac{\varepsilon}{\Gamma_0 a_0} (1 + KM_0)^2 \mathrm{H}_n^{(2)}(\Gamma_0(a_0 + \delta)) - \mathrm{H}_n^{(2)\prime}(\Gamma_0(a_0 + \delta)) \right]} \frac{\mathrm{H}_n^{(2)}(\Gamma_0(a_0 + \delta))}{G} \Bigg]. \tag{11}$$

The rest of the terms are

$$G = \left\{1 + \varepsilon^2 \left[\mu\Big(\frac{s^2}{3g} + \frac{1}{2}\Big) - \nu\Big(\frac{s^2}{4} + \frac{2}{3}g + \frac{1}{2}\frac{g^2}{s^2}\Big)\right]\right\}, \tag{12}$$

and

$$R = \left\{\mu\Big(\frac{1}{g} - \frac{1}{(s^2+g)}\Big) - \nu - \varepsilon\left[\frac{(2n^2-\mu)}{s^2}\ln\Big(\frac{s^2+g}{g}\Big) - \frac{2n^2}{s^2+g} + \frac{\mu}{g} - \frac{\nu}{2}\right]\right\}, \tag{13}$$

where $\nu = (k_0 a_0)^2$, $\mu = (k_0 a_0)^2 K^2 + n^2$, $s = K(M_0 - M_w)$, $g = s(1 + KM_w)$ and $K = \frac{k_z}{k_0}$.

3. Results

This sections includes some illustrative results, including examples of benchmarking that compare results from the theoretical analysis with numerical results taken from Gaffney [12]. Particular focus is given to quantifying the shielding effect upstream of the source. In all of the following examples, the dimensions of the problem and the source characteristics are constant. The fuselage radius is unity ($a_0 = 1$), and the other geometric parameters are scaled by a_0. The Mach number is 0.75 which is a representative value for flight condition at 30,000 ft. The frequency is expressed in terms of the non-dimensional Helmholtz number $k_0 a$, and is fixed at $k_0 a = 20$ which represents a relatively high frequency. Examples are shown for the upstream fuselage pressure, since this is the area expected to produce shielding due to refraction.

In order to quantify the shielding effect on the fuselage surface, the quantity $\Delta_{bl} = \mathrm{SPL}_{bl} - \mathrm{SPL}$ is introduced, which is the difference of the sound pressure level (SPL) with the boundary layer (calculated using eq. (9)) and the SPL without the boundary layer (calculated using eq. (5)). This quantity is particularly relevant at the near side of the cylindrical fuselage ($\bar{\phi} = 0^{\mathrm{o}}$). At the far side of the cylinder (around $\bar{\phi} = 180^{\mathrm{o}}$), there is a shadow zone, and the SPL is typically over 100 dB lower. In fact it is difficult to accurately calculate these very low levels owing to the numerical noise floor, but since the levels are at least 100 dB lower in the shadow zone, this renders the actual levels largely irrelevant.

The key objective underpinning these illustrative results is to show that the linear shear velocity profile can be used to simulate the shielding that is predicted for a 1/7th power-law profile that is a realistic mean-flow profile of a turbulent boundary layer. In order to achieve comparable results, an equivalency must be established between the two profiles. In this paper, three matching methods are investigated to approximate a 1/7th power-law profile by a linear shear profile. The first method is to match the shape factors of the two profiles. Equating the displacement and momentum thicknesses yields values of the boundary-layer thickness δ, and Mach number at the wall M_w, for the equivalent linear shear velocity profile. The second method is to equate the boundary-layer and displacement thicknesses of the two profiles. The third method is to equate the boundary-layer and momentum thicknesses of the two profiles. Figure (2) demonstrates the accuracy of each method, based on a 1/7th power-law profile with actual thickness equal to 1% of the fuselage radius.

It is clear that the best method is to equate the shape factor. The equivalent linear shear velocity profile can simulate the results for a 1/7th power-law profile. By matching the shape factors, the thickness for the equivalent linear shear profile is smaller than the actual boundary-layer thickness of the 1/7th power-law profile. This contributes to the accuracy of the results, because the theoretical approach is valid for sufficiently thin boundary layers compared to the radius of the cylindrical fuselage.

This loss of accuracy with thicker boundary layers is seen in Fig. (3). It is clear that the thicker the boundary layer the larger the discrepancy between the theoretical results and the numerical results. It is important to note here that a typical value for a turbulent boundary-layer thickness at the plane of the source, based on a model of the growth of a turbulent

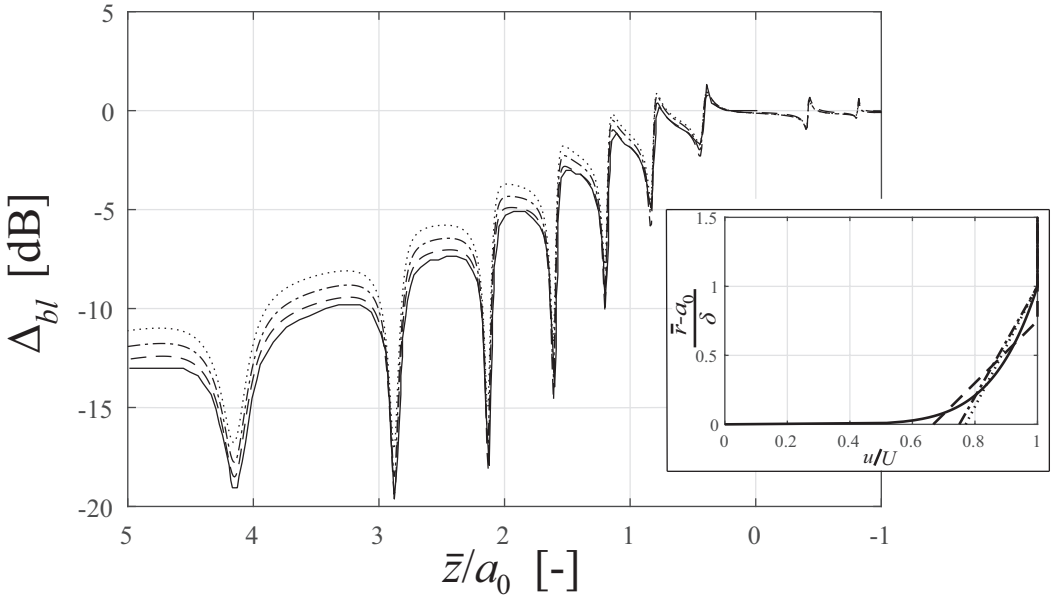

Figure 2. Δ_{bl} at $\bar{\phi} = 0$ for three different matching methods. [**left**] Theoretical predictions with linear velocity profiles having equal shape factor (dashed line), equal boundary-layer and displacement thickness (dash-dotted line), and equal boundary-layer and momentum thickness (dotted line) to a 1/7th power law are compared with numerical predictions (solid line). [**right**] The three equivalent linear velocity profiles, equal shape factor (dashed line), equal boundary-layer and displacement thickness (dash-dotted line), and equal boundary-layer and momentum thickness (dotted line) are plotted compared to the actual 1/7th power law profile (solid line). The other parameters are: $(l, q) = (4, 1)$, $a = 0.5a_0$, $b = 3a_0$, $M_0 = 0.75$, $k_0 a = 20$ and $\delta = 0.01a_0$.

boundary layer on a flat plate, is estimated to be approximately 5% of the fuselage radius, i.e. $\delta/a_0 = 0.05$. It is seen that for thinner boundary-layer thicknesses, that are representative of the actual fuselage boundary-layer thickness upstream of the source plane, the linear shear profile is appropriate to use for predictions of the boundary-layer shielding. This means that predictions of the shielding by a realistic mean-flow profile for a turbulent boundary-layer can be determined using the theoretical method for a linear shear velocity profile, without having to compute numerical results for a power-law profile.

A final illustrative example is shown in Fig. 4 that compares the pressure contours on the cylindrical fuselage calculated with the linear shear profile (using the theoretical method described in this paper) and with a 1/7th power-law profile (using the numerical method developed by Gaffney [12]). Figure 4 shows very good agreement between the theoretical and numerical results. The only noticable differences are located in the shadow zone at the far side of the cylinder. However, the sound levels in the shadow zone are 100 dB lower than the near side, effectively reaching the numerical noise floor rendering comparisons in the shadow zone irrelevant. It is clear that for the near side of the cylinder, the results exhibit remarkable similarity showing that the linear shear velocity profile can be used to calculate the shielding by a 1/7th power-law profile representative of a realistic turbulent boundary layer.

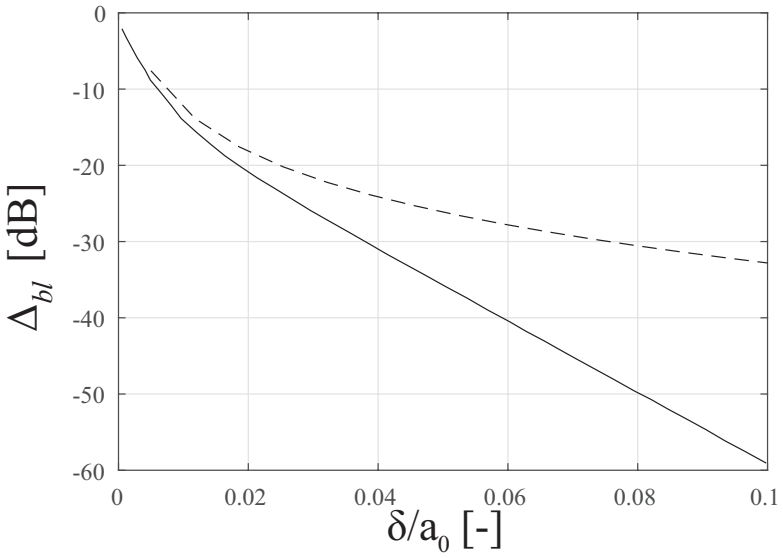

Figure 3. Δ_{bl} at $\bar{\phi} = 0$ and $\bar{z} = 5a_0$ vs boundary-layer thickness. Comparison of theoretical results (dashed line) and numerical results (solid line). The other parameters are: $(l, q) = (4, 1)$, $a = 0.5a_0$, $b = 3a_0$, $M_0 = 0.75$, $k_0a = 20$ and 1/7th power law profile.

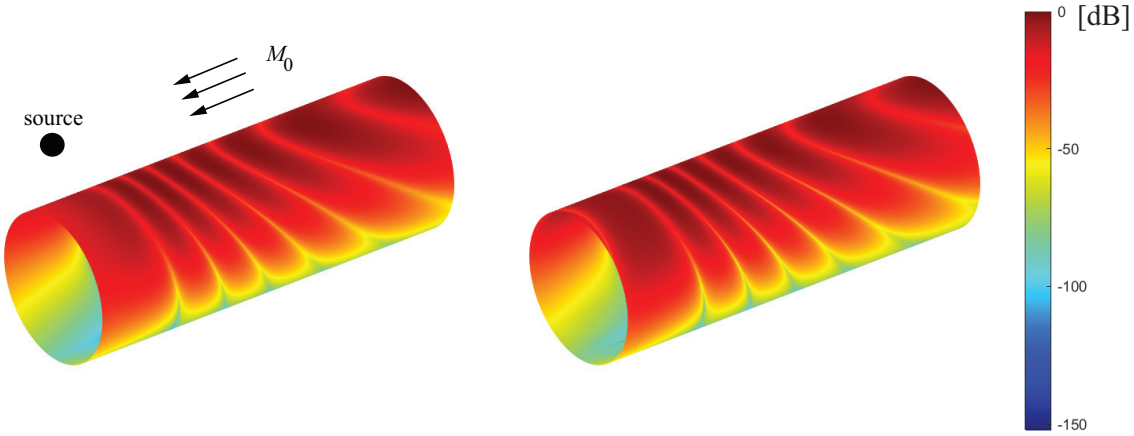

Figure 4. Pressure on the fuselage surface upstream of the source. SPL normalised so that the maximum value is at 0 dB. Comparison of theoretical results **[(right)]** and numerical results **[(left)]**. The other parameters are: $(l, q) = (4, 1)$, $a = 0.5a_0$, $b = 3a_0$, $M_0 = 0.75$, $k_0a = 20$ and 1/7th power law profile.

4. Conclusion

In this paper, a theoretical method for predicting the scattering and shielding effect of a fan tone noise source adjacent to a cylindrical fuselage is developed. Sound propagation through the fuselage boundary layer is calculated using an asymptotic method that is valid for a thin shear layer. Analytical expressions for the acoustic pressure in the near- and far-field have been derived (although only the near-field result is included in this paper). Comparisons with

numerical predictions demonstrate the validity of the approach, and show the feasibility of using an equivalent linear shear velocity profile to accurately approximate a 1/7th power-law velocity profile that is a well-known model of a turbulent boundary layer. The method used for matching the two shear velocity profiles is subject to further investigation. Nonetheless, matching the shape factor is proving to yield accurate results.

The use of the linear shear velocity profile to approximate more realistic profiles implies that perhaps even simpler profiles, such as a step-function velocity profile, could be used to simulate the same results. This would further simplify the problem, eliminating the requirement to solve the Pridmore-Brown equation for sound propagation in the boundary-layer region. The analytical solution for a simpler velocity profile reduces the computational cost of the approach compared to more traditional high-fidelity numerical methods.

Acknowledgments

The work in this paper is part of the ARTEM project. This project has received funding from the European Union's Horizon 2020 research and innovation programme under grant No. 769 350. The first author also acknowledges the financial contribution from the EPSRC via the University of Southampton's Doctoral Training Grant. The authors wish to acknowledge the technical input to this work from Christoph Richter (Rolls–Royce plc) and from James Gaffney. The latter kindly provided use of their installation acoustics code to calculate the numerical results for a 1/7th power-law boundary-layer profile shown in this paper. Also the authors wish to acknowledge the continuing support provided by Rolls–Royce plc through the University Technology Centre in Propulsion Systems Noise at the Institute of Sound and Vibration Research, University of Southampton.

References

[1] D.B. Hanson, "Shielding of prop-fan noise by the fuselage boundary layer", *Journal of Sound and Vibration*, **92**(4), pp. 591-598, 1984.
[2] D.B. Hanson and B. Magliozzi, "Propagation of propeller tone noise through a fuselage boundary layer", *Journal of Aircraft*, **22**(1), pp. 63-70, 1985.
[3] C.R. Fuller, "Free-field correction factor for spherical acoustic waves impinging on cylinders", *American Institute of Aeronautics and Astronautics Journal*, **27**(12), pp. 1722-1726, 1989.
[4] A. McAlpine, J. Gaffney, M.J. Kingan, "Near-field sound radiation of fan tones from an installed turbofan aero-engine", *Journal of Acoustical Society of America*, **138**(3), pp. 1313-1324, 2015.
[5] G.L. McAninch, "A note on propagation through a realistic boundary layer", *Journal of Sound and Vibration*, **88**(2), pp. 271-274, 1983.
[6] C.K.W. Tam and P.J. Morris, "The radiation of sound by the instability waves of a compressible plane turbulent shear layer", *Journal of Fluid Mechanics*, **98**(2), pp. 349-381, 1980.
[7] J. Gaffney, A. McAlpine, M.J. Kingan, "Fuselage boundary-layer refraction of fan tones radiated from an installed turbofan aero-engine", *Journal of Acoustical Society of America*, **141**(3), pp. 1653-1663, 2017.
[8] W. Eversman and R.J. Beckemeyer,"Transmission of sound in ducts with thin shear layers-Convergence to the uniform flow case", *Journal of the Acoustical Society of America*, **52**(1), pp. 216-220, 1972.
[9] D-M. Rouvas and A. McAlpine."Theoretical methods for the prediction of near-field and far-field sound radiation of fan tones scattered by a cylindrical fuselage", *Proceedings of the AIAA Aviation 2021 Forum*, AIAA-2021-2300, August 2–6, 30 pages, `https://doi.org/10.2514/6.2021-2300`.
[10] H.Y. Lu, "Fuselage Boundary-Layer Effects on Sound Propagation and Scattering", *American Institute of Aeronautics and Astronautics Journal*, **28**(7), pp. 1180-1186, 1990.
[11] D. C. Pridmore-Brown,"Sound propagation in a fluid flowing through an attenuating duct", *Journal of Fluid Mechanics*, **4**, pp. 393-406, 1958.
[12] J. Gaffney, *Theoretical Methods to Predict Near-field Fuselage Installation Effects due to Inlet Fan Tones*, Ph.D. thesis, University of Southampton, 2016.